SABA Publishing

Journal of Mathematical Analysis and Modeling
jmam.sabapub.com
ISSN 2709-5924

J Math Anal & Model
(2024)5(2) : 14-43
doi:10.48185/jmam.v5i2.983

Flexural Response of a Cantilever Beam under Masses of Varying Velocities with General Boundary Condition

ADELOYE TO [a,*], OMOLOFE B[b]

[a] Department of Mathematics, Nigeria Maritime University, P.M.B. 1005 Warri
[b] Department of Mathematical Sciences, Federal University of Technology, Akure.

• *Received: 05 January 2024* • *Accepted: 21 June 2024* • *Published Online: 29 June 2024*

Abstract

Response characteristics of an isotropic Rayleigh beam with general boundary constraints under the influence of dynamic loads are explored. A fourth-order partial differential equation describes and governs the behaviour of this problem. The weighted residual method converts the governing equation into a series of coupled second-order type of differential equations to facilitate the analysis. A revised version of Struble's asymptotic method is utilized to simplify the transformed governing equation further. This modification aids in reducing the complexity of the motion equation. The Duhamel integration method is then used to find closed-form solutions to the problem, which are then contrasted for three different force motions: forward force, retard force, and uniform. Essential factors such as prestressed force, foundation subgrade, rotatory inertial correction factor, beam length, and the speed of moving loads are all carefully examined, and their impacts are established in this study.

Keywords: Bi-parametric Elastic Foundation, Response Characteristics, Duhamel Integration, Dynamic Deflections, Travelling time
2010 MSC: 37N15, 74K10, 74H15, 74H50.

1. Introduction

Mathematical modelling is a powerful tool which has been used to investigate the dynamics of several real-life problems, such as infectious diseases, by many mathematicians and researchers [1, 2, 3, 4, 5]. In studying the soil-structure interaction problems, the subject of beams on elastic foundations is fundamental. The dynamic behaviour of elastic systems with moving or static loads has been thoroughly investigated in the science literature with many practical applications in areas like the analysis of buildings, geotechnicals, bridges, highway and railroad structures, submerged pipes, pressure-wave-prone beams, and two-phase flow piping systems.

Researchers have conducted several mathematical investigations and experiments to understand better how structures behave under the influence of moving loads [6, 7, 8,

*Corresponding author: tolulope.adeloye@nmu.edu.ng

9, 10, 11, 12, 13, 14, 15]. However, it is worth noting that most of the studies available in the literature have focused on beams with masses travelling at a constant velocity, limiting the scope of the problem. This is because the vibrating system undergoes non-constant acceleration, deceleration, or uniform motion, leading to more complex dynamic behaviour. Only a few authors in contemporary literature have addressed the problem of flexural vibrations involving a deformable beam under the influence of accelerating loads.

Some notable researchers, including [16], investigated the mechanics of a finite, inextensible beam supported by a homogeneous elastic foundation under accelerating masses. The Galerkin's approach reduces the partial differential equations that describe transient vibrations of the structure-load system to a finite-dimensional problem. The numerical integration method was later used to get convergent solutions of the beam system. He concluded that the reverse force required to stop the mass at a desired point decreases as the friction between the mass and the beam increases.

[17] studied a Rayleigh beam's response under axial prestress, supported by an elastic foundation, and exposed to concentrated masses moving at different velocities. He used the finite Fourier transform method and a modification of Struble's asymptotic approach to solve the beam problem. Practical examples were used to illustrate the proposed analytical procedure, which showed excellent agreement with previous results. [18] investigated the dynamic properties of a structurally prestressed beam under accelerating loads and compressive axial force.

In order to address the problem of structure-load, a method was developed. The method incorporates the integral transformation approach, Struble's asymptotic technique, and Galerkin's residual procedure. Practical examples illustrate the presented theory and analysis, demonstrating how the vibrating system is affected by time-varying velocity. Despite the impressiveness of this research, only boundary conditions with simple support are used as examples. The authors in all the studies above used the basic mechanical foundation model developed by Winkler, commonly known as a one-parameter model, making the solution techniques inapplicable to boundary conditions other than the simple ones. Its drawback lies in its assumption of no interaction between the springs, thus failing to accurately depict the characteristics of numerous practical foundations.

Using eigenfunctions, [19] solved the problem of a heavy mass travelling over a simply supported beam. However, boundary conditions in engineering problems are typically complicated. It is interesting to examine the physics behind the dynamic behaviour of a cantilever and pinned-pinned beam under heavy-moving loads [20], [21], [22].

This study aims to analyze the behaviour of cantilever beams under varying mass velocities and general boundary conditions supported by two-parameter elastic foundations. The main objective is obtaining an analytical solution that applies to all classical boundary conditions for this problem. The study will compare the response of the beam to different types of motion, including accelerating, decelerating, and uniform velocity. It will also consider illustrative examples of simply supported and fixed-free end conditions. The study will investigate the effects of the shear deformation, rotatory inertia correction factor and the foundation modulus on the dynamic characteristics of the structure-load system.

2. Problem Formulation

Examine the bending behaviour of a finite-length Rayleigh beam with homogeneous characteristics. The beam is subjected to an evenly distributed strip load with masses denoted by $\bar{M}$ and is supported on an elastic foundation. The formulation of the equation is non-dimensional and is provided below

$$\frac{\partial^2}{\partial\eta^2}\left[EJ\frac{\partial^2\Theta_z(\eta,t)}{\partial\eta^2}\right]-N\frac{\partial^2\Theta_z(\eta,t)}{\partial\eta^2}+\mu\frac{\partial^2\Theta_z(\eta,t)}{\partial t^2}-\mu R_0\frac{\partial^2\Theta_z(\eta,t)}{\partial\eta^2\partial t^2}+K\Theta_z(\eta,t)$$
$$-G\frac{\partial^2\Theta_z(\eta,t)}{\partial\eta^2}=Q_z(\eta,t) \tag{2.1}$$

The above equation describes the deflection of the beam at a given point in space η and time t. The beam's properties, such as its moment of inertia J and mass per unit length μ, remain constant throughout its length L. The equation incorporates various parameters, including the modulus of elasticity E, the second moment of the beam's cross-section I, the mass per unit length of the beam μ, the prestressed axial force N, the foundation modulus K, the shear rigidity G, the rotatory inertial R_0, and the deflection of the beam from its unloaded equilibrium point is represented by the symbol $\Theta_z(\eta,t)$. Additionally taken into account in the equation is the travelling load of the beam, $Q_z(\eta,t)$. This structure has arbitrary boundary conditions and assumes standard initial conditions without losing generality.

$$\Theta_z(\eta,0)=0=\frac{\partial\Theta_z(\eta,0)}{\partial t} \tag{2.2}$$

and the load

$$Q_z(\eta,t)=P_f(\eta,t)\left[1-\frac{d^2}{dt^2}\left[\frac{\Theta_z(\eta,t)}{g}\right]\right] \tag{2.3}$$

while

$$P_f(\eta,t)=\frac{\bar{M}g}{\chi}[H(\eta-(\tau(t))+\chi)-H(\eta-(\tau(t))-\chi)] \tag{2.4}$$

the property of the Heaviside unity function is expressed as

$$H(\eta)=\begin{cases}0 & \text{if} \quad \eta<0,\\ 1 & \text{if} \quad \eta>0,\end{cases} \tag{2.5}$$

regarding limiting case, $\chi\to 0$,

$$\delta(\eta-(\tau(t)))=\frac{1}{\chi}[H(\eta-(\tau(t))+\chi)-H(\eta-(\tau(t))-\chi)] \tag{2.6}$$

A function that depends on time describes the mass's motion at any given point in time as $\tau(t)=\chi+ct+\frac{1}{2}at^2$, where $\delta(.)$ represents the Dirac delta function. At time $t=0$, the force $Q_z=\bar{M}g$ acts at the point χ, with initial velocity c and constant acceleration a. Additionally, the operator $\frac{d^2}{dt^2}$ in 2.4 is defined in 2.3 as

$$\frac{d^2}{dt^2}\left[\cdot\right]=\left[\frac{\partial^2}{\partial t^2}+2\frac{d}{dt}(\tau(t))\frac{\partial^2}{\partial\eta\partial t}+\left(\frac{d}{dt}(\tau(t))\right)^2\frac{\partial^2}{\partial\eta^2}+\frac{d^2}{dt^2}(\tau(t))\frac{\partial}{\partial\eta}\right]\left[\cdot\right] \tag{2.7}$$

2.1 can be simplified by taking into account equations 2.4 through 2.5 and 2.7

$$\frac{\partial^2}{\partial\eta^2}\left[EJ\frac{\partial^2\Theta_z(\eta,t)}{\partial\eta^2}\right]-N\frac{\partial^2\Theta_z(\eta,t)}{\partial\eta^2}+\mu\frac{\partial^2\Theta_z(\eta,t)}{\partial\eta^2}-\mu R_0\frac{\partial^2\Theta_z(\eta,t)}{\partial\eta^2\partial t^2}+K\Theta_z(\eta,t)-G\frac{\partial^2\Theta_z(\eta,t)}{\partial\eta^2}$$
$$=\frac{\bar{M}g}{\chi}\left[H(\eta-(\tau(t))+\chi)-H(\eta-(\tau(t))-\chi)\right]-\frac{\bar{M}}{\chi}\left[H(\eta-(\tau(t))+\chi)-H(\eta-(\tau(t))-\chi)\right]$$
$$\left[\frac{\partial^2\Theta_z(\eta,t)}{\partial t^2}+2\frac{d}{dt}(\tau(t))\frac{\partial^2\Theta_z(\eta,t)}{\partial\eta\partial t}+\left(\frac{d}{dt}(\tau(t))\right)^2\frac{\partial^2\Theta_z(\eta,t)}{\partial\eta^2}+\frac{d^2}{dt^2}(\tau(t))\frac{\partial\Theta_z(\eta,t)}{\partial\eta}\right] \tag{2.8}$$

2.8 governs the motion of a prismatic Rayleigh beam under axial compression and accelerating loads.

3. Solution Procedure

Consider

$$\Theta_z(\eta,t)=\sum_{m=1}^{\infty}Y_z(t)U_z(\eta) \tag{3.1}$$

To solve problems involving mechanical vibrations, the Weighted Residual Method, a versatile technique, will be adopted.

$$U_z(\eta)=\sin\frac{\iota_z\eta}{L}+\Upsilon_{1m}\cos\frac{\iota_z\eta}{L}+\Upsilon_{2m}\sinh\frac{\iota_z\eta}{L}+\Upsilon_{3m}\cosh\frac{\iota_z\eta}{L} \tag{3.2}$$

The mode frequency ι_z and the constants Υ_{1m}, Υ_{2m}, and Υ_{3m} determine the $z-th$ normal mode of vibration of a uniform beam function. These constants can be obtained by substituting 3.2 with appropriate boundary conditions. It should be noted that for a simply supported beam, $\Upsilon_{1m}=\Upsilon_{2m}=\Upsilon_{3m}=0$ and $\iota_z=m\pi$.
The technique for solving the problem requires that 2.8 is expressed as

$$\Omega(\eta,t)=\sum_{m=1}^{\infty}Y_z(t)U_z(\eta) \tag{3.3}$$

2.8 in view of 3.3 becomes

$$\ddot{Y}_z(t)+\gamma_{mf}^2 Y_z(t)+\Gamma\sum_{m=1}^{\infty} J_6^{\star}\Bigg[\Bigg[U_z(f(t))U_n(f(t))+\frac{\chi^2}{6}\Big(U_z(f(t))U_n''(f(t))+U_z''(f(t))U_n(f(t))$$

$$+((f(t)))'(f(t))U_n'(f(t))\Big)\Bigg]\ddot{Y}_z(t)+2(c+at)\Bigg[U_z(f(t))U_n(f(t))+\frac{\chi^2}{6}\Big(U_z(f(t))U_n''(f(t))$$

$$+U_z''(f(t))U_n(f(t))+((f(t)))'(f(t))U_n'(f(t))\Big)\Bigg]\dot{Y}_z(t)+(c+at)^2\Bigg[U_z''(f(t))U_n(f(t))$$

$$+\frac{\chi^2}{6}\Big(U_z^{iv}(f(t))U_n(f(t))+U_z''(f(t))U_n''(f(t))+((f(t)))'''(f(t))U_n'(f(t))\Big)\Bigg]Y_z(t)$$

$$+a\Bigg[U_z'(f(t))U_n(f(t))+\frac{\chi^2}{6}\Big(U_z'''(f(t))U_n(f(t))+U_z'(f(t))U_n''(f(t))$$

$$+((f(t)))''(f(t))U_n'(f(t))\Big)\Bigg]Y_z(t)\Bigg]=\frac{\bar{M}g}{\mu(J_1-R_0J_2)}\Bigg[U_z(f(t))+\frac{\chi^2}{6}U_z''(f(t))\Bigg] \tag{3.4}$$

where

$$J_1=\int_0^L U_z(x)U_n(x)dx \qquad J_2=\int_0^L U_z''(x)U_n(xx \qquad J_3=\int_0^L U_z^{iv}(x)U_n(x)dx$$

$$J_4=\int_0^L U_z''(x)U_n(x)dx \qquad J_5=\int_0^L U_z(x)U_n(x)dx \qquad J_6=\int_0^L U_z''(x)U_n(x)dx \tag{3.5}$$

$$\Gamma=\frac{\bar{M}}{\mu L} \qquad \text{and} \qquad \gamma_{mf}^2=\frac{EIJ_3-NJ_4+KJ_5-GJ_6}{\mu(J_1-R_0J_2)} \tag{3.6}$$

the transformed equation governing the vibration problem of a prismatic beam is represented by 3.4. This beam is traversed by partially distributed accelerating masses. The coupled non-homogeneous second-order ordinary differential equation applies to all variants of classical boundary conditions. In the following, we will consider two exceptional cases of 3.4.

3.1. Case I: The Effect of a Moving Force on Prismatic Rayleigh Beam

In 3.4, setting Γ to zero can be used to derive the differential equation that describes the response of a prismatic Rayleigh beam with an elastic foundation to a moving force with a varying velocity.

$$\ddot{Y}_z(t)+\gamma_{mf}^2 Y_z(t)=P_z\Bigg[a_1\sin\frac{\iota_z}{L}(\chi+ct+\frac{1}{2}at^2)+a_2\cos\frac{\iota_z}{L}(\chi+ct+\frac{1}{2}at^2)$$

$$+a_3\sinh\frac{\iota_z}{L}(\chi+ct+\frac{1}{2}at^2)+a_4\cosh\frac{\iota_z}{L}(\chi+ct+\frac{1}{2}at^2)\Bigg] \tag{3.7}$$

to solve 3.7 use is made of the impulse response function given as

$$Y_z(t) = \int_0^t \theta_z(t-\tau)P_z(\tau)d\tau \tag{3.8}$$

where

$$\theta_z(t) = \begin{cases} \frac{1}{\omega_{bm}} e^{-\varepsilon_z \omega_z t} \sin \omega_{bm} t & \text{if} \quad t \geqslant 0, \\ 0 & \text{if} \quad t < 0, \end{cases} \tag{3.9}$$

and

$$\omega_{bm} = \omega_z \sqrt{1-\varepsilon_z^2} \tag{3.10}$$

is the damped circular frequency of the mth mode of the beam. Since the effect of damping parameters is insignificant for analyzing dynamic response [18], we set $\varepsilon_z = 0$ and $\omega_{bm} = \omega_z$. The solution of 3.7 may be written as

$$\begin{aligned} Y_z(t) = & \frac{P_z}{\gamma_{mf}} \Bigg\{ a_1 \int_0^t \sin \gamma_{mf}(t-\tau) \sin \omega(\chi + c\tau + \frac{1}{2}a\tau^2)d\tau \\ & + a_2 \int_0^t \sin \gamma_{mf}(t-\tau) \cos \omega(\chi + c\tau + \frac{1}{2}a\tau^2)d\tau \\ & + a_3 \int_0^t \sin \gamma_{mf}(t-\tau) \sinh \omega(\chi + c\tau + \frac{1}{2}a\tau^2)d\tau \\ & + a_4 \int_0^t \sin \gamma_{mf}(t-\tau) \cosh \omega(\chi + c\tau + \frac{1}{2}a\tau^2)d\tau \Bigg\} \end{aligned} \tag{3.11}$$

where

$$\omega = \frac{\iota_z}{L} \quad , P_z = \frac{\bar{M}g}{\mu(J_1 - R_0 J_2)} \tag{3.12}$$

Thus, in view of 3.1 taking into account 3.11, we have

$$\Theta(\eta,t)=\sum_{m=1}^{\infty}\frac{P_z}{\gamma_{mf}}\left\{\frac{a_1+a_2i}{4(1-i)}\sqrt{\frac{\pi}{a\omega}}\left[\operatorname{erf}\left(\frac{(1-i)(\omega at+c\omega+\gamma_{mf})}{2\sqrt{a\omega}}\right)-\operatorname{erf}\left(\frac{(1-i)(c\omega+\gamma_{mf})}{2\sqrt{a\omega}}\right)\right.\right.$$

$$\left(\cos m_2-i\sin m_2\right)-\left(\operatorname{erf}\left(\frac{(1-i)(\omega at+c\omega-\gamma_{mf})}{2\sqrt{a\omega}}\right)-\operatorname{erf}\left(\frac{(1-i)(c\omega-\gamma_{mf})}{2\sqrt{a\omega}}\right)\right)$$

$$\left.\left(\cos m_1+i\sin m_1\right)\right]-\frac{(a_1-a_2i)(1-i)}{8}\sqrt{\frac{\pi}{a\omega}}\left[\operatorname{erf}\left(\frac{(1+i)(\omega at+c\omega-\gamma_{mf})}{2\sqrt{a\omega}}\right)\right.$$

$$-\operatorname{erf}\left(\frac{(1+i)(c\omega-\gamma_{mf})}{2\sqrt{a\omega}}\right)\left(\cos m_3-i\sin m_3\right)-\left(\operatorname{erf}\left(\frac{(1+i)(\omega at+c\omega+\gamma_{mf})}{2\sqrt{a\omega}}\right)\right.$$

$$\left.\left.-\operatorname{erf}\left(\frac{(1+i)(c\omega+\gamma_{mf})}{2\sqrt{a\omega}}\right)\right)\left(\cos m_4+i\sin m_4\right)\right]\Bigg]-\frac{a_3+a_4}{4}\sqrt{\frac{\pi}{2a\omega}}\left[\left(\operatorname{erf}\left(\frac{i\gamma_{mf}-\omega at-\omega c}{i\sqrt{2a\omega}}\right)\right.\right.$$

$$\left.\left.-\operatorname{erf}\left(\frac{i\gamma_{mf}-\omega c}{i\sqrt{a\omega}}\right)\right)e^{m_5}+\left(\operatorname{erf}\left(\frac{\omega at+i\gamma_{mf}+c\omega}{i\sqrt{2a\omega}}\right)-\operatorname{erf}\left(\frac{c\omega+i\gamma_{mf}}{i\sqrt{2a\omega}}\right)\right)e^{m_6}\right]$$

$$-\frac{a_3-a_4}{8i}\frac{1}{2}\sqrt{\frac{2\pi}{a\omega}}\left[\left(\operatorname{erf}\left(\frac{1}{2}\sqrt{\frac{2}{a\omega}}\left(i\gamma_{mf}-\omega at-\omega c\right)\right)-\operatorname{erf}\left(\frac{1}{2}\sqrt{\frac{2}{a\omega}}\left(i\gamma_{mf}-\omega c\right)\right)\right)e^{m_7}\right.$$

$$\left.+\left(\operatorname{erf}\left(\frac{1}{2}\sqrt{\frac{2}{a\omega}}\left(\omega at-i\gamma_{mf}+\omega c\right)\right)-\operatorname{erf}\left(\frac{1}{2}\sqrt{\frac{2}{a\omega}}\left(\omega c+i\gamma_{mf}\right)\right)\right)e^{m_8}\right]\Bigg\}\times$$

$$\left[\sin\frac{\iota_z x}{L}+\Upsilon_{1m}\cos\frac{\iota_z x}{L}+\Upsilon_{2m}\sinh\frac{\iota_z x}{L}+\Upsilon_{3m}\cosh\frac{\iota_z x}{L}\right] \tag{3.13}$$

3.13 explains how a structurally prestressed beam reacts to accelerating or decelerating forces. Similarly, the dynamic response of an axially prestressed thick beam to uniform velocity forces can be easily determined as shown below

$$\begin{aligned}\Theta_z(\eta,t)=\sum_{m=1}^{\infty}\frac{P_z}{\gamma_{mf}\left(\gamma_{mf}^4-\omega^4\right)}&\left\{z_1\left(\gamma_{mf}^2+\omega^2\right)\left(\gamma_{mf}\sin\omega t-\omega\sin\gamma_{mf}t\right)\right.\\&+z_3\left(\gamma_{mf}^2-\omega^2\right)\left(\gamma_{mf}\sinh\omega t-\omega\sin\gamma_{mf}t\right)+z_2\gamma_{mf}\left(\gamma_{mf}^2+\omega^2\right)\left(\cos\omega t-\cos\gamma_{mf}t\right)\\&\left.+z_4\gamma_{mf}\left(\gamma_{mf}^2-\omega^2\right)\left(\cosh\omega t-\cos\gamma_{mf}t\right)\right\}\times\\&\left[\sin\frac{\iota_z x}{L}+\Upsilon_{1m}\cos\frac{\iota_z x}{L}+\Upsilon_{2m}\sinh\frac{\iota_z x}{L}+\Upsilon_{3m}\cosh\frac{\iota_z x}{L}\right]\end{aligned} \tag{3.14}$$

where

$$z_1 = 1 - \frac{1}{6}\left(\frac{\chi \iota_z c}{L}\right)^2, \qquad z_2 = \Upsilon_{1m} - \frac{\Upsilon_{1m}}{6}\left(\frac{\chi \iota_z c}{L}\right)^2$$

$$z_3 = \Upsilon_{2m} + \frac{\Upsilon_{2m}}{6}\left(\frac{\chi \iota_z c}{L}\right)^2, \qquad z_4 = \Upsilon_{3m} + \frac{\Upsilon_{3m}}{6}\left(\frac{\chi \iota_z c}{L}\right)^2 \tag{3.15}$$

3.2. Case II: The Effect of a Moving Mass on Prismatic Rayleigh Beam

The considerable influence of the load's inertia occurs when the mass of the moving load is similar to that of the structure. As a result, the solution of the complete 3.4 becomes necessary, and Γ is no longer zero. This scenario is known as the moving mass problem. Since obtaining a closed-form solution for 3.4 is not feasible, an approximate analytical approach called the Struble method is used. 3.4 is recast as follows

$$\ddot{Y}_z(t) + \frac{2\Gamma J_6^\star (c+at)\left\{U_4 + \frac{\chi^2}{6}\left[U_5 + 3U_6\right]\right\}}{1 + \Gamma J_6^\star\left\{U_1 + \frac{\chi^2}{3}\left[U_2 + U_3\right]\right\}}\dot{Y}_z(t)$$

$$+ \frac{\gamma_{mf}^2 + \Gamma J_6^\star (c+at)^2\left\{U_2 + \frac{\chi^2}{6}\left[U_7 + U_8 + U_9\right] + a\Gamma J_6^\star\left[U_4 + \frac{\chi^2}{6}\left[U_5 + 3U_6\right]\right]\right\}}{1 + \Gamma J_6^\star\left\{U_1 + \frac{\chi^2}{3}\left[U_2 + U_3\right]\right\}} Y_z(t)$$

$$+ \sum_{\substack{m=1 \\ m\neq n}}^{\infty} \frac{\Gamma J_6^\star\left\{U_{10} + \frac{\chi^2}{6}\left[U_{11} + U_{12} + 2U_{13}\right]\right\}}{1 + \Gamma J_6^\star\left\{U_1 + \frac{\chi^2}{3}\left[U_2 + U_3\right]\right\}}\ddot{Y}_z(t)$$

$$+ \frac{2(c+at)\Gamma J_6^\star\left\{U_{14} + \frac{\chi^2}{6}\left[U_{15} + U_{16} + 2U_{17}\right]\right\}}{1 + \Gamma J_6^\star\left\{U_1 + \frac{\chi^2}{3}\left[U_2 + U_3\right]\right\}}\dot{Y}_z(t)$$

$$+ \frac{(c+at)^2\Gamma J_6^\star\left\{U_{12} + \frac{\chi^2}{6}\left[U_{18} + U_{19} + 2U_{20}\right]\right\} + a\Gamma J_6^\star\left\{U_{14} + \frac{\chi^2}{6}\left[U_{15} + U_{16} + 2U_{17}\right]\right\}}{1 + \Gamma J_6^\star\left\{U_1 + \frac{\chi^2}{3}\left[U_2 + U_3\right]\right\}} Y_z(t)$$

$$= \frac{\frac{\Gamma g L}{J_7}\left\{U_z(f(t)) + \frac{\chi^2}{6}U_z''(f(t))\right\}}{1 + \Gamma J_6^\star\left\{U_1 + \frac{\chi^2}{3}\left[U_2 + U_3\right]\right\}} \tag{3.16}$$

For 3.16, there is no definite analytical solution, unlike the prismatic Rayleigh beam problem in instance I. Therefore, the Struble technique, a variant of the asymptotic approach, is used to solve weakly homogeneous and non-homogeneous non-linear oscillatory equations. Using this method, we find a modified natural frequency associated with the free system frequency influenced by the moving mass. 3.16, then, is replaced by the operator of an analogous free system, defined by the modified frequency. Thus, for any arbitrary mass ratio, we set the right-hand component of 3.16 to zero and introduce a parameter $\Gamma^\star < 1$.

$$\Gamma^\star = \frac{\Gamma}{1+\Gamma} \tag{3.17}$$

It can be shown that

$$\Gamma = \Gamma^\star\left[1 + O(\Gamma) + O(\Gamma^2) + \ldots\right] \tag{3.18}$$

and

$$\frac{1}{1+\Gamma J_6^\star\left\{U_1 + \frac{\chi^2}{3}\left[U_2+U_3\right]\right\}} = 1 - \Gamma^\star J_6^\star\left\{U_1 + \frac{\chi^2}{3}\left[U_2+U_3\right]\right\} \tag{3.19}$$

where

$$\left|J_6^\star\left\{U_1 + \frac{\chi^2}{3}\left[U_2+U_3\right]\right\}\right| < 1 \tag{3.20}$$

substituting 3.18 and 3.19 into 3.16 we have

$$\ddot{Y}_z(t) + 2\Gamma^\star J_6^\star(c+at)\left\{U_4 + \frac{\chi^2}{6}\left[U_5+3U_6\right]\right]\right\}\dot{Y}_z(t) + \left\{\gamma_{mf}^2 - \gamma_{mf}^2\Gamma^\star J_6^\star\left\{U_1 + \frac{\chi^2}{3}\left[U_2+U_3\right]\right\}\right.$$

$$\left. + \Gamma^\star J_6^\star(c+at)^2\left\{U_2 + \frac{\chi^2}{6}\left[U_7+U_8+U_9\right]\right\} + a\Gamma^\star J_6^\star\left\{U_4 + \frac{\chi^2}{6}\left[U_5+3U6\right]\right\}\right\}Y_z(t)$$

$$+ \sum_{\substack{m=1\\m\neq n}}^{\infty}\Gamma^\star J_6^\star\left\{U_{10} + \frac{\chi^2}{6}\left[U_{11}+U_{12}+2U_{13}\right]\right\}\ddot{Y}_z(t)$$

$$+ 2(c+at)\Gamma^\star J_6^\star\left\{U_{14} + \frac{\chi^2}{6}\left[U_{15}+U_{16}+2U_{17}\right]\right\}\dot{Y}_z(t)$$

$$+ \left\{\Gamma^\star J_6^\star(c+at)^2\left\{U_{12} + \frac{\chi^2}{6}\left[U_{18}+U_{19}+2U_{20}\right]\right\}\right.$$

$$\left. + a\Gamma^\star J_6^\star\left\{U_{14} + \frac{\chi^2}{6}\left[U_{15}+U_{16}+2U_{17}\right]\right\}Y_z(t)\right\} = \frac{\Gamma^\star gL}{J_7}\left\{U_z(f(t)) + \frac{\chi^2}{6}U_z''(f(t))\right\} \tag{3.21}$$

when $\Gamma^\star$ is set to zero in 3.21, the result corresponds to the case where the inertial effect of the system's mass is disregarded. Subsequently, the homogeneous part of the 3.21 transforms as follows

$$\ddot{Y}_z(t) + \gamma_{mf}^2 Y_z(t) = 0 \tag{3.22}$$

it is simple to show that the solution to 3.22 can be obtained from this harmonic differential equation

$$Y_z(t) = \Upsilon_{1m}(t)\cos(\gamma_{mf}t - \phi_z t) \tag{3.23}$$

However, we always have $\Gamma^\star < 1$ for any arbitrary mass ratio Γ. Consequently, the homogenous part of the 3.21 can be represented asymptotically as

$$Y_z(t) = \Upsilon_{1m}(t)\cos(\gamma_{mf}t - \phi_z(t)) + \Gamma^\star Y_z(t) + O(\Gamma^\star)^2 \tag{3.24}$$

3.21 simplifies to when the homogeneous parts of the equation is replaced by 3.24 and its first and second derivatives, and non-contributing terms are ignored in the variational equations

$$\begin{aligned}
&-2\gamma_{mf}\dot{A}_z(t)\sin(\gamma_{mf}t - \phi_z(t)) \\
&2\Upsilon_{1m}(t)\dot{\phi}_z(t)\cos(\gamma_{mf}t - \phi_z(t)) \\
&-\gamma_{mf}^2\Upsilon_{1m}(t)\cos(\gamma_{mf}t - \phi_z(t)) \\
&-2\Upsilon_{1m}(t)\gamma_{mf}\Gamma^\star J_6^\star c\left\{U_4 + \frac{\chi^2}{6}\left[U_5 + 3U_6\right]\right\}\sin(\gamma_{mf}t - \phi_z(t)) \\
&\gamma_{mf}^2\Upsilon_{1m}(t)\cos(\gamma_{mf}t - \phi_z(t)) \\
&-\gamma_{mf}^2\Gamma^\star J_6^\star\Upsilon_{1m}(t)\left\{U_1 + \frac{\chi^2}{3}\left[U_2 + U_3\right]\right\}\cos(\gamma_{mf}t - \phi_z(t)) \\
&\Gamma^\star J_6^\star c^2\Upsilon_{1m}(t)\left\{U_2 + \frac{\chi^2}{6}\left[U_7 + U_8 + U_9\right]\right\}\cos(\gamma_{mf}t - \phi_z(t)) \\
&a\Gamma^\star J_6^\star\Upsilon_{1m}(t)\left\{U_4 + \frac{\chi^2}{6}\left[U_5 + 3U_6\right]\right\}\cos(\gamma_{mf}t - \phi_z(t)) \\
&= 0
\end{aligned} \tag{3.25}$$

setting $\cos(\gamma_{mf}t - \phi_z(t))$ and $\sin(\gamma_{mf}t - \phi_z(t))$ to zero on the right side of 3.25 gives us

$$-2\gamma_{mf}\dot{A}_z(t) - 2\Upsilon_{1m}(t)\gamma_{mf}\Gamma^\star J_6^\star c\left\{U_4 + \frac{\chi^2}{6}\left[U_5 + 3U_6\right]\right\} = 0 \tag{3.26}$$

and

$$\begin{aligned}
&2\Upsilon_{1m}(t)\dot{\phi}_z(t) - \gamma_{mf}^2\Upsilon_{1m}(t) + \gamma_{mf}^2\Upsilon_{1m}(t) - \gamma_{mf}^2\Gamma^\star J_6^\star\Upsilon_{1m}(t)\left\{U_1 + \frac{\chi^2}{3}\left[U_2 + U_3\right]\right\} \\
&+ \Gamma^\star J_6^\star c^2\Upsilon_{1m}(t)\left\{U_2 + \frac{\chi^2}{6}\left[U_7 + U_8 + U_9\right]\right\} + a\Gamma^\star J_6^\star\Upsilon_{1m}(t)\left\{U_4 + \frac{\chi^2}{6}\left[U_5 + 3U_6\right]\right\} = 0
\end{aligned} \tag{3.27}$$

Evaluating 3.26 and 3.27 one obtains

$$\Upsilon_{1m}(t) = \Theta_z e^{\Gamma^\star J_6^\star c\left\{U_4+\frac{\chi^2}{6}\left[U_5+3U_6\right]\right\}t} \tag{3.28}$$

where Θ_z =constant and

$$\begin{aligned}\phi_z(t) =&\frac{\Gamma^\star J_6^\star}{2}\left\{\gamma_{mf}\left[U_1+\frac{\chi^2}{3}\left[U_2+U_3\right]\right]-\frac{1}{\gamma_{mf}}\left[c^2\left\{U_2+\frac{\chi^2}{6}\left[U_7+U_8+U_9\right]\right\}\right]\right.\\ &\left.+a\left\{U_4+\frac{\chi^2}{6}\left[U_5+3U_6\right]\right\}\right\}t+\phi_z\end{aligned} \tag{3.29}$$

substituting 3.28 and 3.29 , one obtains

$$\begin{aligned}Y_z(t) =&\Theta_z e^{\Gamma^\star J_6^\star c\left\{U_4+\frac{\chi^2}{6}\left[U_5+3U_6\right]\right\}t}\cos\left\{\gamma_{mf}t-\frac{\Gamma^\star J_6^\star}{2}\left\{\gamma_{mf}\left[U_1+\frac{\chi^2}{3}\left[U_2+U_3\right]\right]\right.\right.\\ &\left.\left.-\frac{1}{\gamma_{mf}}\left[c^2\left\{U_2+\frac{\chi^2}{6}\left[U_7+U_8+U_9\right]\right\}\right]+a\left\{U_4+\frac{\chi^2}{6}\left[U_5+3U_6\right]\right\}\right\}t+\phi_z\right\}\end{aligned} \tag{3.30}$$

which after some arrangements yields

$$Y_z(t) = \Theta e^{\Gamma^\star J_6^\star c\left\{U_4+\frac{\chi^2}{6}\left[U_5+3U_6\right]\right\}t}\cos(\gamma_{mm}t-\phi_z) \tag{3.31}$$

where

$$\begin{aligned}\gamma_{mm} =&\gamma_{mf}\left\{1-\frac{\Gamma^\star J_6^\star}{2\gamma_{mf}^2}\left\{\gamma_{mf}^2\left[U_1+\frac{\chi^2}{3}\left[U_2+U_3\right]\right]-c^2\left\{U_2+\frac{\chi^2}{6}\left[U_7+U_8+U_9\right]\right\}\right.\right.\\ &\left.\left.-a\left\{U_4+\frac{\chi^2}{6}\left[U_5+3U_6\right]\right\}\right\}\right\}\end{aligned} \tag{3.32}$$

The free system frequency influenced by the presence of the moving mass is the modified natural frequency, represented by 3.32. Consequently, we may express the homogeneous component of 3.22 as

$$\ddot{Y}_z(t)+\gamma_{mm}^2 Y_z(t) = 0 \tag{3.33}$$

Consequently, the entire 3.21 now becomes

$$\begin{aligned}\ddot{Y}_z(t)+\gamma_{mm}^2 Y_z(t) =&P_z\left[a_1\sin\frac{\iota_z}{L}(\chi+ct+\frac{1}{2}at^2)+a_2\cos\frac{\iota_z}{L}(\chi+ct+\frac{1}{2}at^2)\right.\\ &\left.+a_3\sinh\frac{\iota_z}{L}(\chi+ct+\frac{1}{2}at^2)+a_4\cosh\frac{\iota_z}{L}(\chi+ct+\frac{1}{2}at^2)\right]\end{aligned} \tag{3.34}$$

where

$$P_z = \frac{\Gamma^\star gL}{J_7} \tag{3.35}$$

3.34 is analogous to 3.7 and following similar arguments one obtains

$$Y_z(t) = \frac{P_z}{\gamma_{mm}}\left\{ a_1 \int_0^t \sin\gamma_{mm}(t-\tau)\sin\omega(\chi + c\tau + \frac{1}{2}a\tau^2)d\tau \right.$$

$$+ a_2 \int_0^t \sin\gamma_{mm}(t-\tau)\cos\omega(\chi + c\tau + \frac{1}{2}a\tau^2)d\tau$$

$$+ a_3 \int_0^t \sin\gamma_{mm}(t-\tau)\sinh\omega(\chi + c\tau + \frac{1}{2}a\tau^2)d\tau$$

$$\left. + a_4 \int_0^t \sin\gamma_{mm}(t-\tau)\cosh\omega(\chi + c\tau + \frac{1}{2}a\tau^2)d\tau \right\} \quad (3.36)$$

Thus, in view of 3.1 taking into account 3.36, one obtains

$$\Theta_z(\eta,t)=\sum_{m=1}^{\infty}\frac{P_z}{\gamma_{mm}}\left\{\frac{a_1+a_2i}{4(1-i)}\sqrt{\frac{\pi}{a\omega}}\left[\operatorname{erf}\left(\frac{(1-i)(\omega at+c\omega+\gamma_{mm})}{2\sqrt{a\omega}}\right)-\operatorname{erf}\left(\frac{(1-i)(c\omega+\gamma_{mm})}{2\sqrt{a\omega}}\right)\right.\right.$$

$$\left(\cos m_2-i\sin m_2\right)-\left(\operatorname{erf}\left(\frac{(1-i)(\omega at+c\omega-\gamma_{mm})}{2\sqrt{a\omega}}\right)-\operatorname{erf}\left(\frac{(1-i)(c\omega-\gamma_{mm})}{2\sqrt{a\omega}}\right)\right)$$

$$\left.\left(\cos m_1+i\sin m_1\right)\right]-\frac{(a_1-a_2i)(1-i)}{8}\sqrt{\frac{\pi}{a\omega}}\left[\operatorname{erf}\left(\frac{(1+i)(\omega at+c\omega-\gamma_{mm})}{2\sqrt{a\omega}}\right)\right.$$

$$-\operatorname{erf}\left(\frac{(1+i)(c\omega-\gamma_{mm})}{2\sqrt{a\omega}}\right)\left(\cos m_3-i\sin m_3\right)-\left(\operatorname{erf}\left(\frac{(1+i)(\omega at+c\omega+\gamma_{mm})}{2\sqrt{a\omega}}\right)\right.$$

$$\left.\left.-\operatorname{erf}\left(\frac{(1+i)(c\omega+\gamma_{mm})}{2\sqrt{a\omega}}\right)\right)\left(\cos m_4+i\sin m_4\right)\right]\Big]-\frac{a_3+a_4}{4}\sqrt{\frac{\pi}{2a\omega}}\left[\left(\operatorname{erf}\left(\frac{i\gamma_{mm}-\omega at-\omega c}{i\sqrt{2a\omega}}\right)\right.\right.$$

$$\left.-\operatorname{erf}\left(\frac{i\gamma_{mm}-\omega c}{i\sqrt{a\omega}}\right)\right)e^{m_5}+\left(\operatorname{erf}\left(\frac{\omega at+i\gamma_{mm}+cw}{i\sqrt{2a\omega}}\right)-\operatorname{erf}\left(\frac{c\omega+i\gamma_{mm}}{i\sqrt{2a\omega}}\right)\right)e^{m_6}\Big]$$

$$-\frac{a_3-a_4}{8i}\frac{1}{2}\sqrt{\frac{2\pi}{a\omega}}\left[\left(\operatorname{erf}\left(\frac{1}{2}\sqrt{\frac{2}{a\omega}}\left(i\gamma_{mm}-\omega at-\omega c\right)\right)-\operatorname{erf}\left(\frac{1}{2}\sqrt{\frac{2}{a\omega}}\left(i\gamma_{mm}-\omega c\right)\right)\right)e^{m_7}\right.$$

$$\left.+\left(\operatorname{erf}\left(\frac{1}{2}\sqrt{\frac{2}{a\omega}}\left(\omega at-i\gamma_{mm}+\omega c\right)\right)-\operatorname{erf}\left(\frac{1}{2}\sqrt{\frac{2}{a\omega}}\left(\omega c+i\gamma_{mm}\right)\right)\right)e^{m_8}\right]\Big\}\times$$

$$\left[\sin\frac{\iota_z x}{L}+\Upsilon_{1m}\cos\frac{\iota_z x}{L}+\Upsilon_{2m}\sinh\frac{\iota_z x}{L}+\Upsilon_{3m}\cosh\frac{\iota_z x}{L}\right] \tag{3.37}$$

expression 3.37 illustrates the lateral displacement response of a prismatic beam with an elastic foundation subjected to both prestressed axial force and accelerating loads, independent of the conventional boundary conditions.

Likewise, the deflection of the beam subjected to loads moving with uniform velocity

can be determined as follows

$$\Theta_z(\eta,t)=\sum_{m=1}^{\infty}\frac{P_{mm}}{\gamma_{mm}\left(\gamma_{mm}^4-\omega^4\right)}\Big\{z_1\left(\gamma_{mm}^2+\omega^2\right)\left(\gamma_{mm}\sin\omega t-\omega\sin\gamma_{mm}t\right)$$
$$+z_3\left(\gamma_{mm}^2-\omega^2\right)\left(\gamma_{mm}\sinh\omega t-\omega\sin\gamma_{mm}t\right)$$
$$+z_2\gamma_{mm}\left(\gamma_{mm}^2+\omega^2\right)\left(\cos\omega t-\cos\gamma_{mm}t\right)$$
$$+z_4\gamma_{mm}\left(\gamma_{mm}^2-\omega^2\right)\left(\cosh\omega t-\cos\gamma_{mm}t\right)\Big\}\times$$
$$\left[\sin\frac{\iota_z x}{L}+\Upsilon_{1m}\cos\frac{\iota_z x}{L}+\Upsilon_{2m}\sinh\frac{\iota_z x}{L}+\Upsilon_{3m}\cosh\frac{\iota_z x}{L}\right] \tag{3.38}$$

where

$$P_{mm}=\frac{\Gamma^* gL}{J_7} \tag{3.39}$$

4. Results and Discussions

A homogeneous beam with the following parameter is given as an example: The mass per unit length of the beam is $\mu = 2758.291\text{kg/m}$. The modulus of elasticity is $E = 3.1\times 10^{10}\text{N/m}^2$; the moment of inertial is $J = 2.87698\times 10^{-}3\text{m}^4$; the beam span is $L = 50\text{m}$. The foundation modulus values for this beam vary from 0N/m^3 to 40000N/m^3, whereas the axial force N ranges between 0N and $2.0\times 10^8\text{N}$.

4.1. Pinned-pinned End Condition

Figure 1 shows the deflection amplitude of a simply supported prismatic Rayleigh beam under accelerating forces for various values of axial force N and fixed values of foundation modulus $K = 40000$, shear modulus $G = 300000$ and Rotatory inertia correction factor $R_0 = 50$. It is seen from the figure that as N increases, the dynamic amplitude of deflection of the uniform Rayleigh beam decreases. Similar results are obtained when the simply supported beam is subjected to partially distributed masses travelling at variable velocity, as shown in figure 7.

For various travelling time t, the transverse displacements of the simply supported beam under travelling accelerating forces for various values of foundation modulus K and fixed values of axial force $N = 200000$ and Rotatory inertia correction factor $R_0 = 50$ are shown in figure 2. Higher values of foundation modulus are noted to diminish the dynamic amplitude of deflections in the vibrating beam. The same behaviour characterizes the deflection of the same beam under the action of distributed masses moving at variable velocity for various values of foundation modulus K, as shown in figure 8.

Similarly, figure 3 displays the response amplitudes of the simply supported uniform Rayleigh beam under distributed accelerating forces travelling at variable velocity for various values of shear modulus G and for fixed values of axial force $N = 200000$ and foundation modulus $K = 40000$ and rotatory inertia factor R_0. It is seen from the figure that as G increases, the dynamic amplitude of deflection of the uniform Rayleigh beam decreases. Similar results are obtained when the simply supported uniform beam is subjected to partially distributed masses travelling at variable velocity, as shown in figure 9.

Figures 4 and 10 demonstrate the deflection curves of a simply supported prismatic Rayleigh beam under the influence of accelerating forces and masses, respectively. The curves show the relationship between the deflection and the crossing time for different values of the rotatory inertial factor R_0 while keeping the axial force $N = 200000$, foundation modulus $K = 40000$, shear modulus $G = 30000$ and rotatory inertia factor R_0 constant. The findings indicate that the amplitude of the beam's deflection decreases with an increase in the rotatory inertia factor.

Figures 5 and 11 show the dynamic deflections of a simply supported prismatic Rayleigh beam. The figures depict the beam's deflections as an accelerating force crosses it at various values of the span length L. The axial force N, foundation modulus K, shear modulus G, and rotatory inertia factor R_0 are fixed. As the span length L values increase, the amplitude of deflections in the beam decreases. These figures demonstrate this relationship.

Figures 6 and 12 illustrate the deflection curves versus crossing time for a simply supported prismatic Rayleigh beam subjected to accelerating forces and masses, respectively, at different values of the travelling velocity c and fixed values of axial force $N = 200000$, foundation modulus $K = 40000$, shear modulus $G = 30000$, and rotatory inertia factor R_0. The results indicate that the beams' deflection amplitude decreases as the travelling velocity increases.

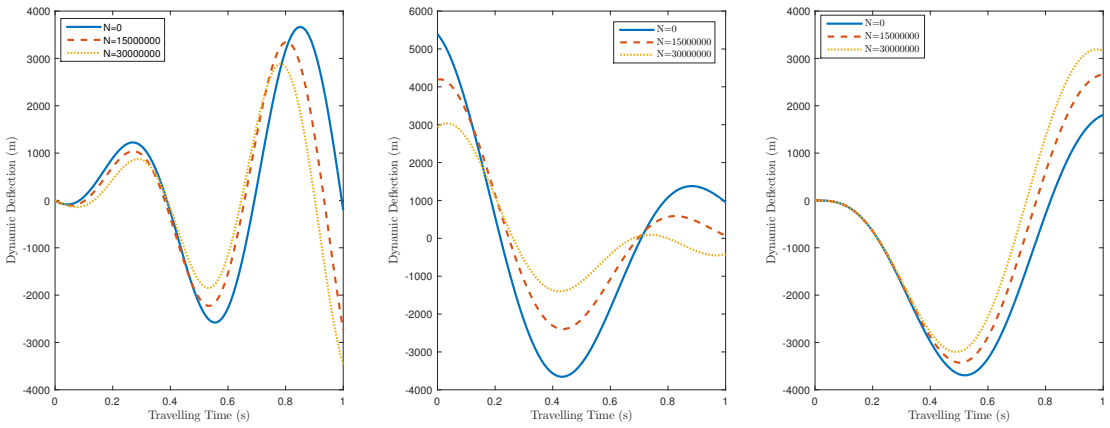

(a) accelerated motion ($a > 0$) (b) decelerated motion ($a < 0$) (c) uniform motion ($a = 0$)

Figure 1: Deformation patterns of a prismatic Rayleigh beam with simple support under increasing forces for different axial force values N and constant foundation modulus values $K = 40000$, shear modulus values $G = 30000$, and rotatory inertial values $R_0 = 20$.

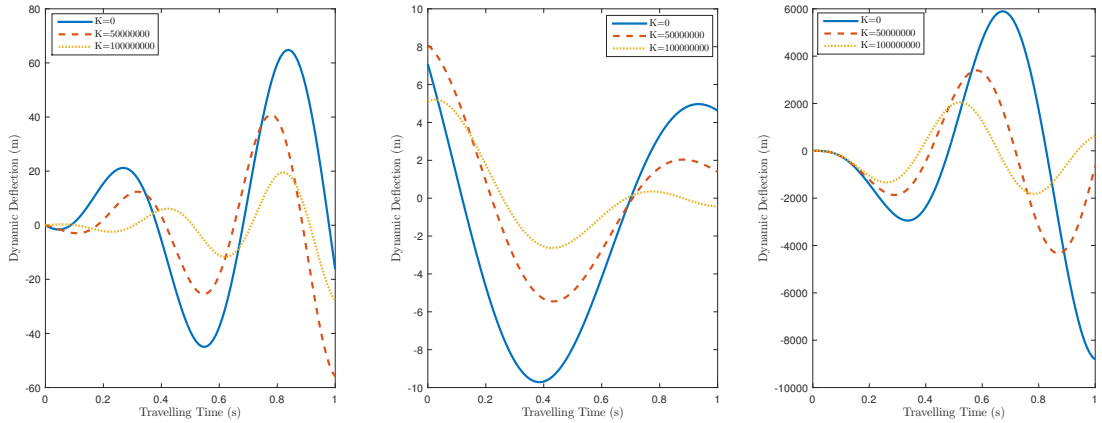

(a) accelerated motion ($\alpha > 0$) (b) decelerated motion ($\alpha < 0$) (c) uniform motion ($\alpha = 0$)

Figure 2: Transverse displacements under accelerating forces of a simply supported prismatic Rayleigh beam for a range of foundation modulus values K, as well as fixed values of axial force N = 40000, shear modulus G = 30000, and rotatory inertial $R_0 = 20$.

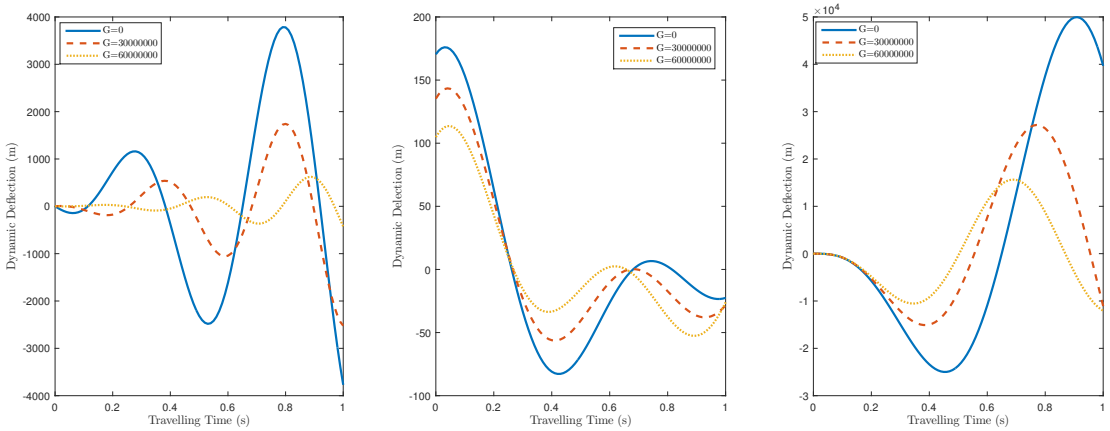

(a) accelerated motion ($\alpha > 0$) (b) decelerated motion ($\alpha < 0$) (c) uniform motion ($\alpha = 0$)

Figure 3: Response amplitudes of a simply supported prismatic Rayleigh beam under accelearting forces for various values of shear modulus G and for fixed values of axial force N = 20000 foundation modulus K = 40000, and rotatory inertial $R_0 = 20$

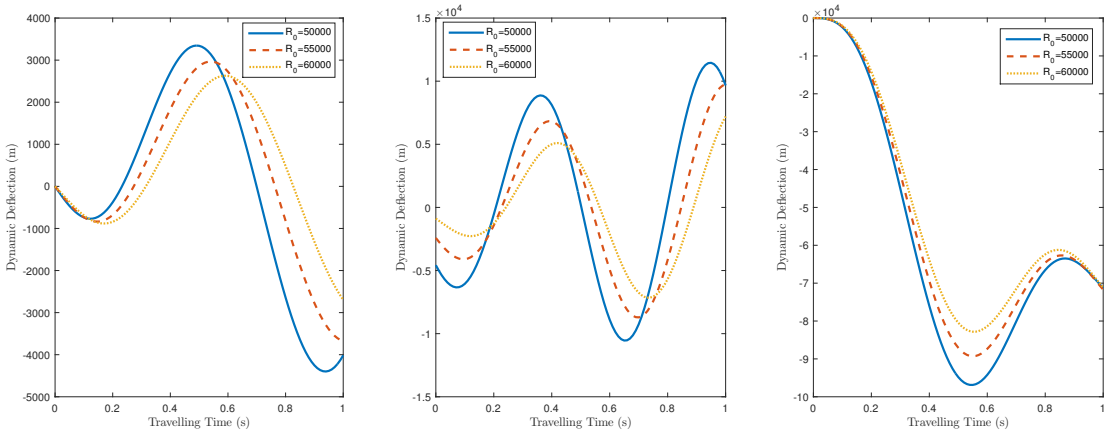

(a) accelerated motion ($\alpha > 0$) (b) decelerated motion ($\alpha < 0$) (c) uniform motion ($\alpha = 0$)

Figure 4: Deflection variation at the mid-span of a simply supported prismatic Rayleigh beam under accelerating forces for various values of rotatory inertial factor R_0 and for fixed values of axial force N, foundation modulus $K = 40000$, shear modulus $G = 30000$

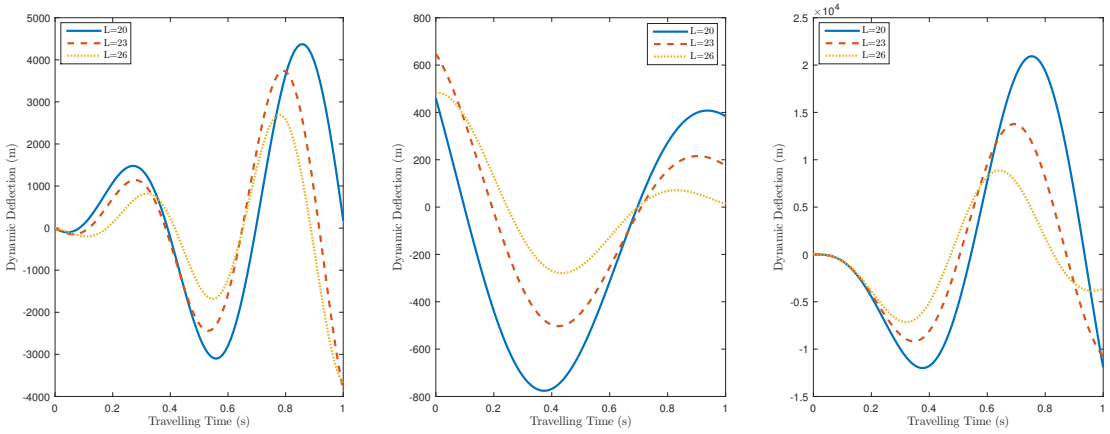

(a) accelerated motion ($\alpha > 0$) (b) decelerated motion ($\alpha < 0$) (c) uniform motion ($\alpha = 0$)

Figure 5: Simple supported prismatic Rayleigh beam dynamic deflections versus the crossing time of an accelerating force for a range of span lengths L and fixed values of the axial force N, foundation modulus $K = 40000$, shear modulus $G = 30000$, and rotatory inertial R_0.

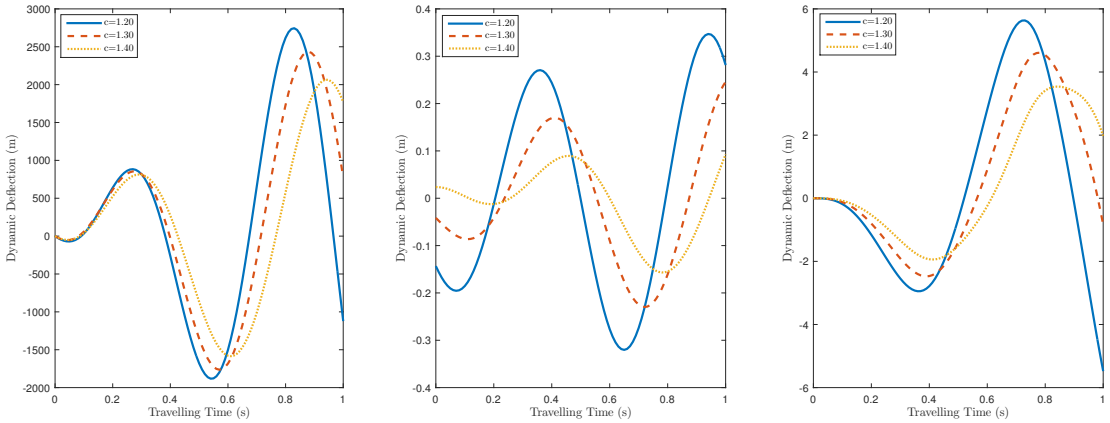

(a) accelerated motion ($\alpha > 0$) (b) decelerated motion ($\alpha < 0$) (c) uniform motion ($\alpha = 0$)

Figure 6: Deflection curves of the simply supported prismatic Rayleigh beam vs the crossing time of an accelearting forces for varied values of the travelling velocities and fixed values of axial force N, rotatory inertial factor R_0, shear modulus G = 30000, foundation modulus K = 40000, and

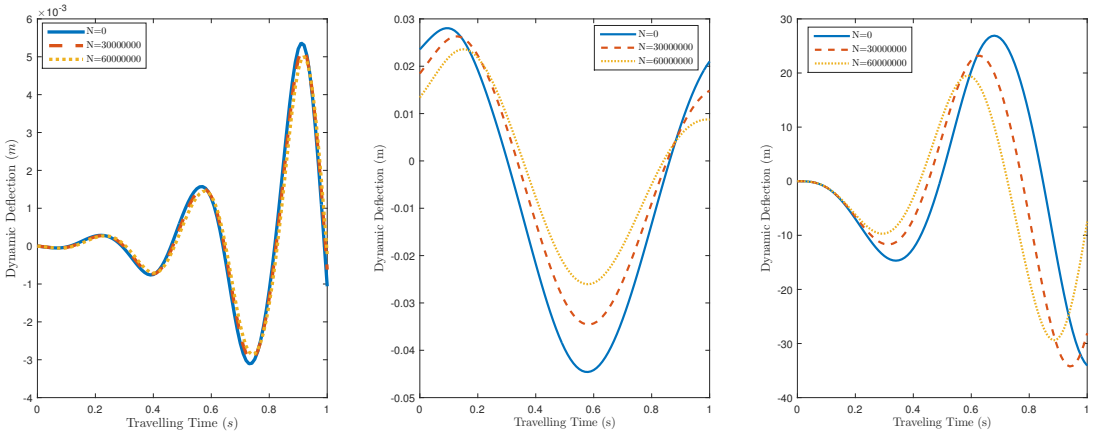

(a) accelerated motion ($\alpha > 0$) (b) decelerated motion ($\alpha < 0$) (c) uniform motion ($\alpha = 0$)

Figure 7: Deformation sequences of a prismatic Rayleigh beam with simple support under increasing weights for different axial force values N and constant foundation modulus values K = 40000, shear modulus values G = 30000, and rotatory inertial values $R_0 = 20$.

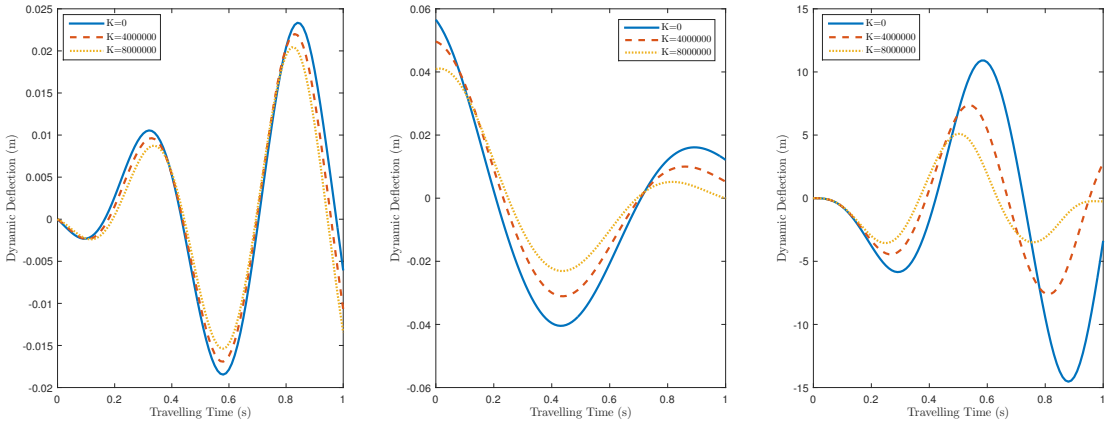

(a) accelerated motion ($\alpha > 0$) (b) decelerated motion ($\alpha < 0$) (c) uniform motion ($\alpha = 0$)

Figure 8: Range of foundation modulus values K for simple support prismatic Rayleigh beam transverse displacements under accelerating masses with fixed values of axial force N = 40000, shear modulus G = 30000, and rotatory inertial $R_0 = 20$.

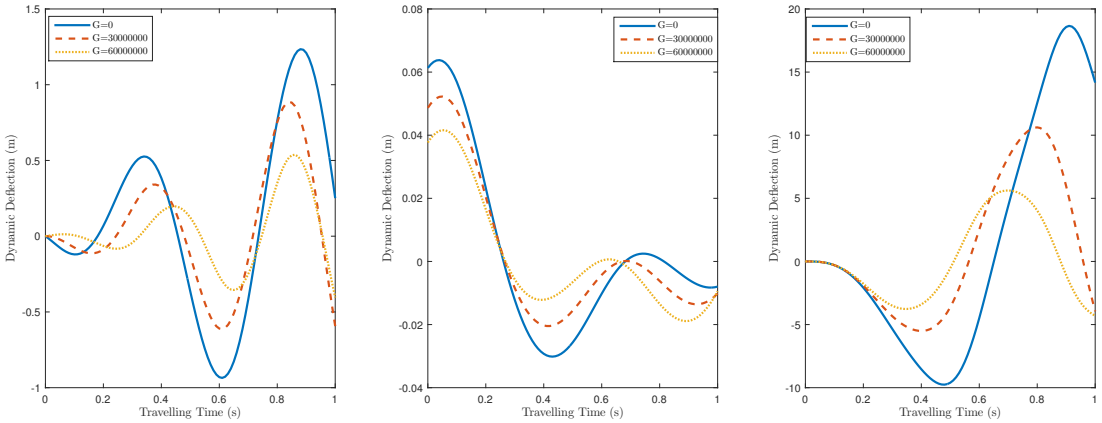

(a) accelerated motion ($\alpha > 0$) (b) decelerated motion ($\alpha < 0$) (c) uniform motion ($\alpha = 0$)

Figure 9: Response amplitudes of a simply supported prismatic Rayleigh beam under accelearting masses for various values of shear modulus G and for fixed values of axial force N = 20000 foundation modulus K = 40000, and rotatory inertial $R_0 = 20$

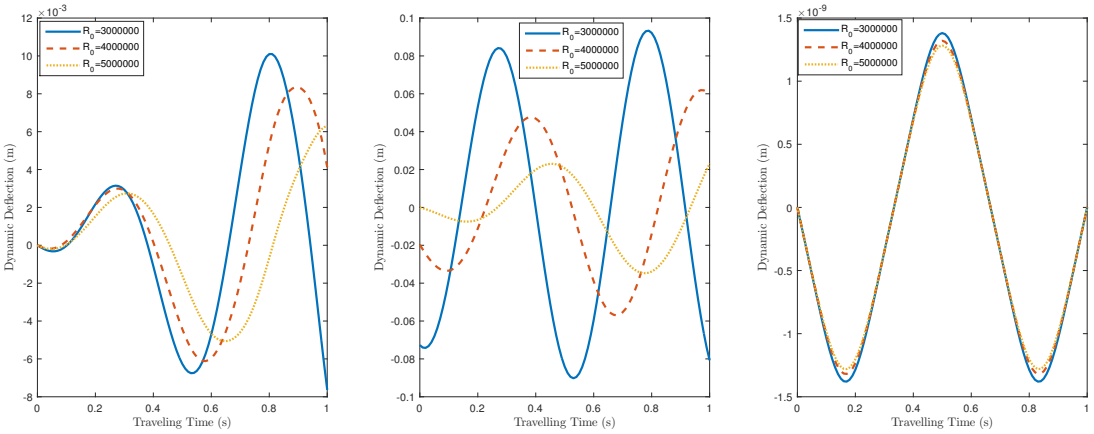

(a) accelerated motion ($\alpha > 0$) (b) decelerated motion ($\alpha < 0$) (c) uniform motion ($\alpha = 0$)

Figure 10: Variations in deflection at the midspan of a simply supported prismatic Rayleigh beam under acceleration masses over a range of rotatory inertial factor values R_0 and for axial force, foundation modulus, and shear modulus fixed values N, $K = 40000$, and $G = 30000$.

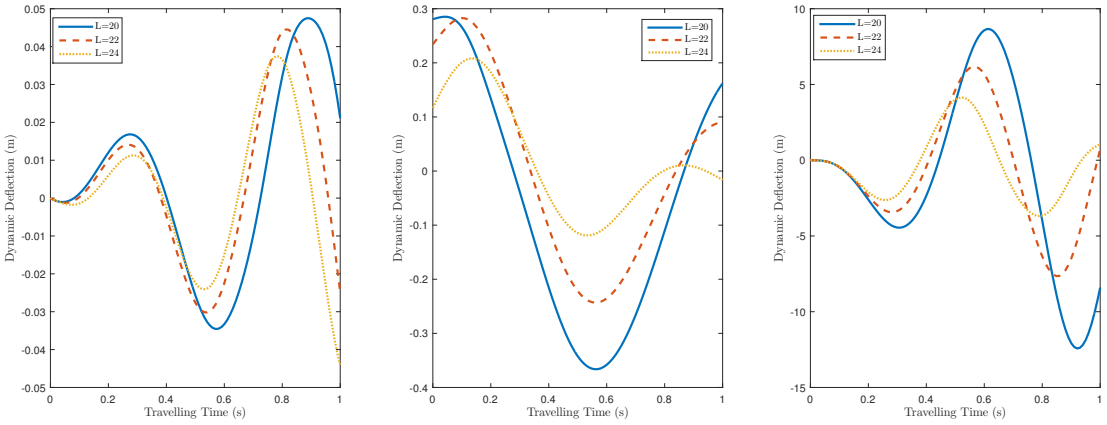

(a) accelerated motion ($\alpha > 0$) (b) decelerated motion ($\alpha < 0$) (c) uniform motion ($\alpha = 0$)

Figure 11: Simple supported prismatic Rayleigh beam dynamic distribution versus the crossing time of accelerating masses for a range of span lengths L and fixed values of the axial force N, foundation modulus $K = 40000$, shear modulus $G = 30000$, and rotatory inertial R_0.

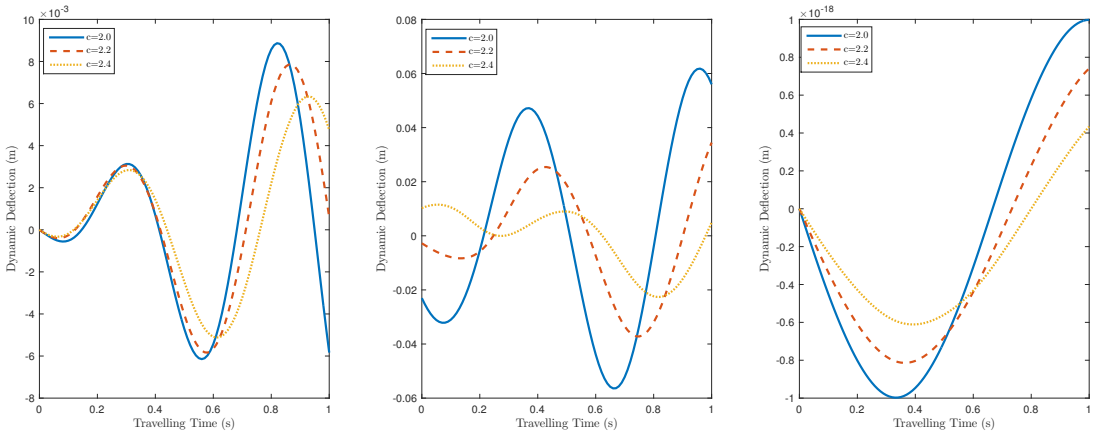

(a) accelerated motion ($a > 0$) (b) decelerated motion ($a < 0$) (c) uniform motion ($a = 0$)

Figure 12: Deformation curves of a prismatic Rayleigh beam with simple support to the crossing time of an accelerating mass, given a range of travelling velocities and constant values of the axial force N, foundation modulus $K = 40000$, shear modulus $G = 30000$, and rotatory inertial factor R_0

4.2. Fixed-free End Condition

The deflection profiles of a prismatic Rayleigh beam with simple support are shown in figure 13. The profiles are displayed for a variety of axial force values, denoted as N, while the foundation modulus, K, shear modulus, G, and rotational inertia correction factor, R_0, are held constant at values of 40000, 300000, and 50, respectively. It is seen from the figure that as N increases, the dynamic amplitude of deflection of the uniform Rayleigh beam decreases. Similar results are obtained when the simply supported beam is subjected to partially distributed masses travelling at variable velocity, as shown in figure 19.

For various travelling time t, the transverse displacements of the simply supported beam under travelling accelerating forces for various values of foundation modulus K and fixed values of axial force $N = 200000$ and Rotatory inertia correction factor $R_0 = 50$ are shown in figure 14. It is found that the dynamic amplitude of deflections in the vibrating beam decreases as the foundation modulus values increases. The same behaviour characterizes the deflection of the same beam under the action of distributed masses moving at variable velocity for various values of foundation modulus K, as shown in figure 20.

Similarly, figure 15 displays the response amplitudes of the simply supported uniform Rayleigh beam under distributed accelerating forces travelling at variable velocity for various values of shear modulus G and for fixed values of axial force $N = 200000$ and foundation modulus $K = 40000$ and rotatory inertia factor R_0. The graphic shows that the dynamic amplitude of deflection of the uniform Rayleigh beam decreases with increasing G. Figure 21 shows comparable outcomes when partially distributed masses moving at varying velocities are applied to the supported uniform beam.

Similarly, for a simply supported prismatic Rayleigh beam acted upon by accelerating forces and masses, respectively, figures 16 and 22 show the deflection curves versus the crossing time for a range of values of the rotatory inertial factor R_0 and fixed values of axial force $N = 200000$, foundation modulus $K = 40000$, shear modulus $G = 30000$, and rotatory inertia factor R_0. It is demonstrated that the magnitude of the beams' deflection reduces as the rotatory inertia factor rises.

Figures 17 and 23 depict, respectively, the dynamic deflections of a simply supported prismatic Rayleigh beam versus the crossing time of accelerating forces for a range of span length values L and fixed values of axial force $N = 200000$, foundation modulus $K = 40000$, shear modulus $G = 30000$, and rotatory inertia factor R_0. These graphs clearly show that as the values of the span length L increase, the beam amplitude of deflections decreases.

Similarly, figures 18 and 24 show the deflection curves versus the crossing time for a range of travelling velocity c and for fixed values of axial force $N = 200000$, foundation modulus $K = 40000$, shear modulus $G = 30000$, and rotatory inertia factor R_0 for a simply supported prismatic Rayleigh beam acted upon by accelerating forces and masses, respectively. It is shown that as the travelling velocity increases, the beams' deflection magnitude increases.

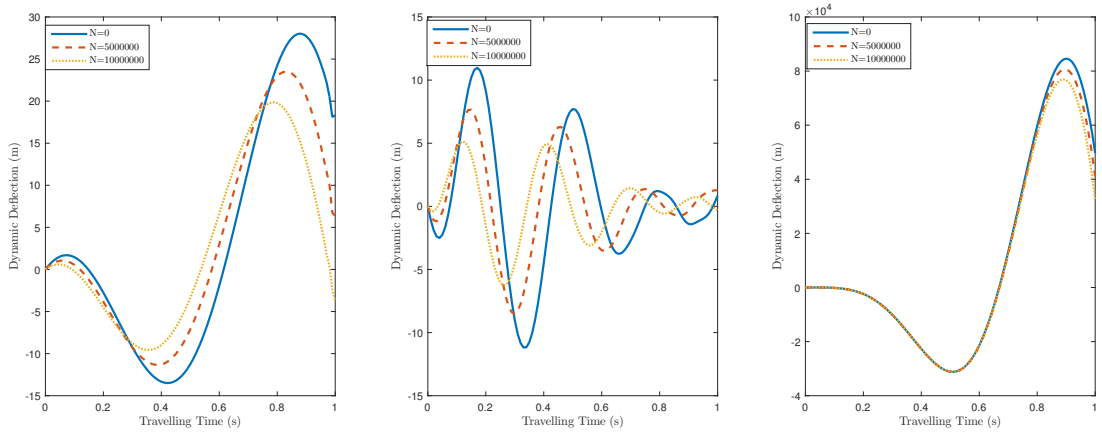

(a) accelerated motion ($\alpha > 0$) (b) decelerated motion ($\alpha < 0$) (c) uniform motion ($\alpha = 0$)

Figure 13: Profiles of deflection of a fixed-free prismatic Rayleigh beam under acceleration forces over a range of axial force values N as well as for fixed values of rotatory inertial $R_0 = 20$, foundation modulus K $= 40000$, and shear modulus G $= 30000$.

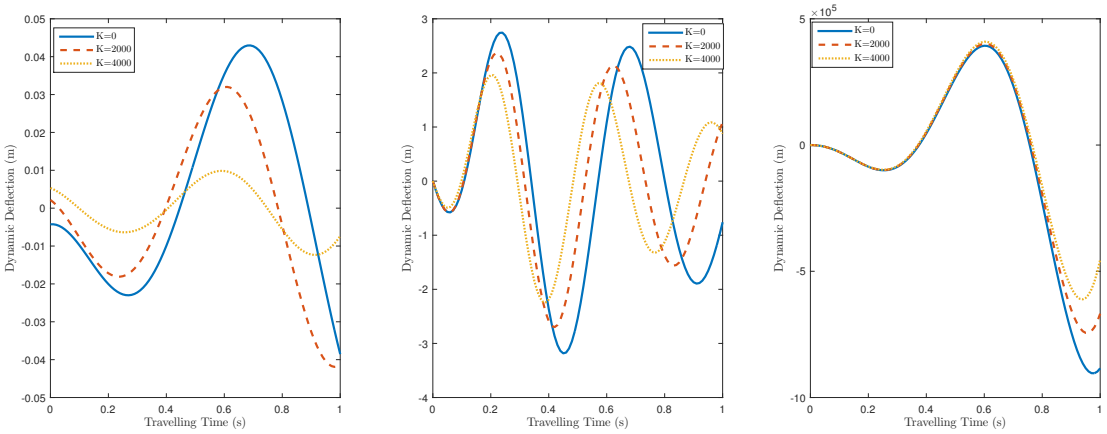

(a) accelerated motion ($\alpha > 0$) (b) decelerated motion ($\alpha < 0$) (c) uniform motion ($\alpha > 0$)

Figure 14: A fixed-free prismatic Rayleigh beam's transverse displacements under accelerating forces over a range of foundation modulus values K, as well as fixed values of axial force (N $= 40000$), shear modulus G $= 30000$, and rotatory inertial $R_0 = 20$.

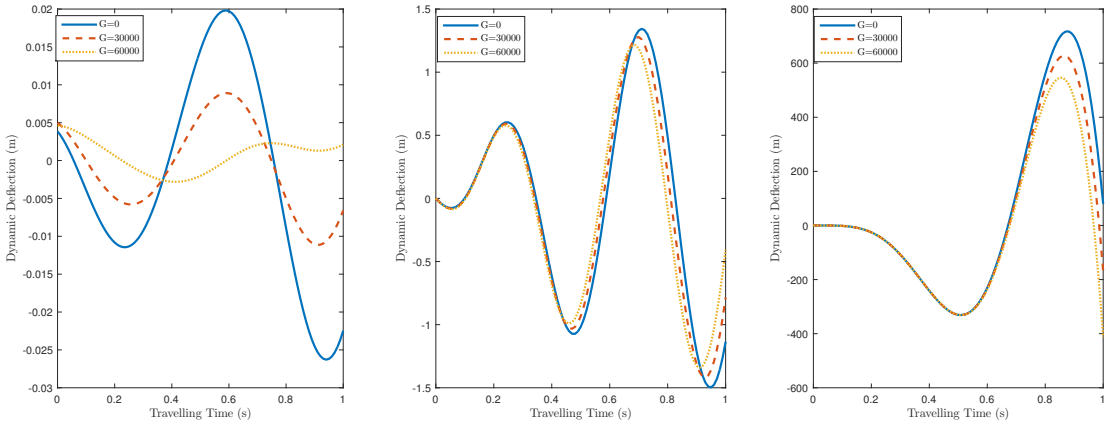

(a) accelerated motion ($\alpha > 0$) (b) decelerated motion ($\alpha < 0$) (c) uniform motion ($\alpha = 0$)

Figure 15: A fixed-free prismatic Rayleigh beam's response amplitudes to accelerating forces with a range of shear modulus values (G), fixed axial force values N = 20000, foundation modulus values K = 40000, and rotatory inertial $R_0 = 20$

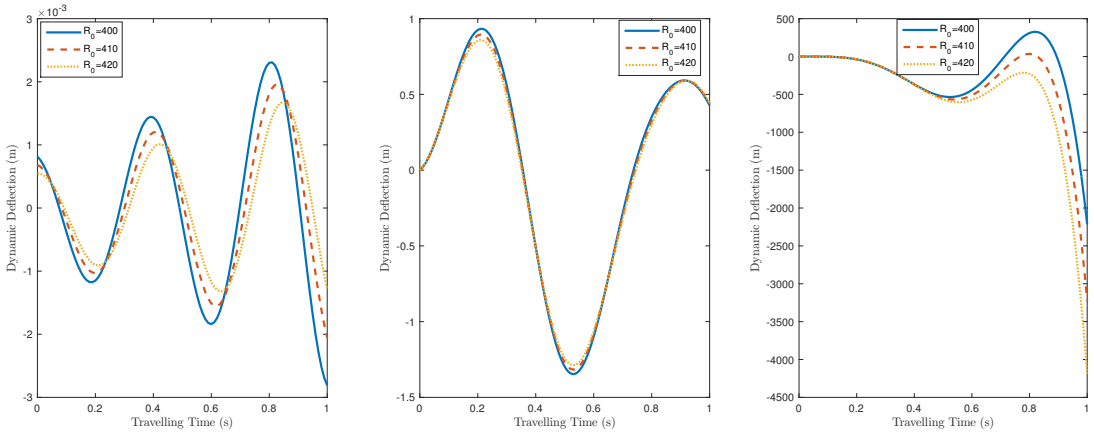

(a) accelerated motion ($\alpha > 0$) (b) decelerated motion ($\alpha < 0$) (c) uniform motion ($\alpha = 0$)

Figure 16: Deflection variations at the mid-span of a fixed-free prismatic Rayleigh beam under accelearting forces for various values of rotatory inertial factor R_0 and for fixed values of axial force N, foundation modulus K = 40000, shear modulus G = 30000

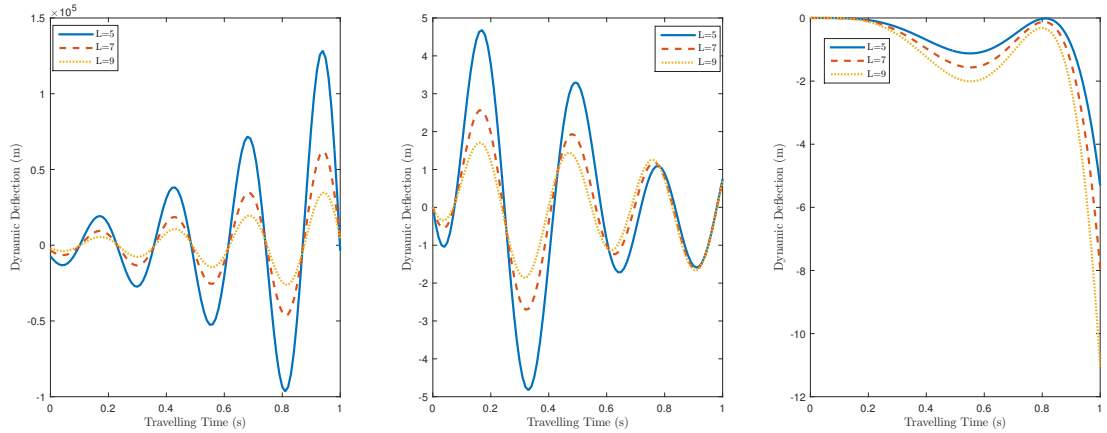

(a) accelerated motion ($\alpha > 0$) (b) decelerated motion ($\alpha < 0$) (c) uniform motion ($\alpha = 0$)

Figure 17: Different values of the span length L and fixed values of the axial force N, foundation modulus K = 40000, shear modulus G = 30000, and rotatory inertial R_0, the dynamic deflections of a fixed-free prismatic Rayleigh beam vs the crossing time of an accelerating force

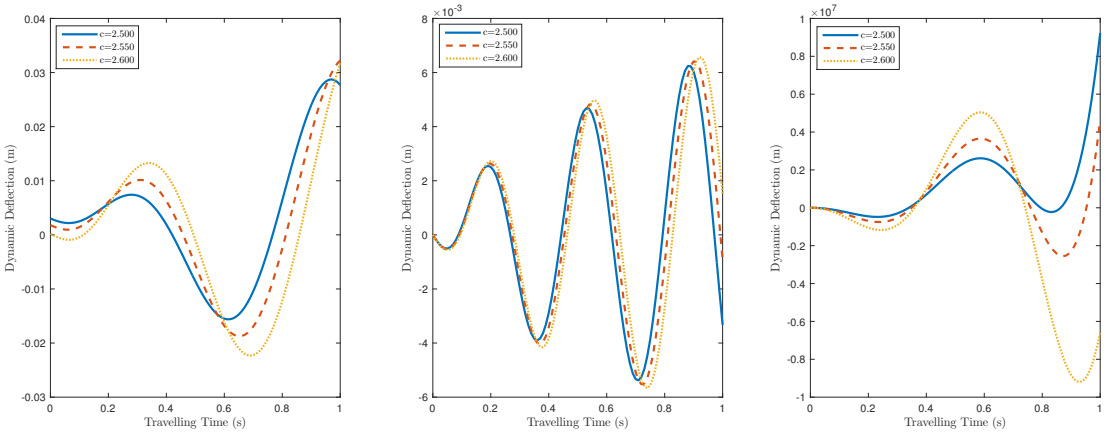

(a) accelerated motion ($\alpha > 0$) (b) decelerated motion ($\alpha < 0$) (c) uniform motion ($\alpha = 0$)

Figure 18: Deflection distribution of a fixed-free prismatic Rayleigh beam for different travelling velocities and fixed axial force values vs the crossing time of an accelerating force N, rotatory inertial factor R_0, shear modulus G = 30000 and foundation modulus K = 40000

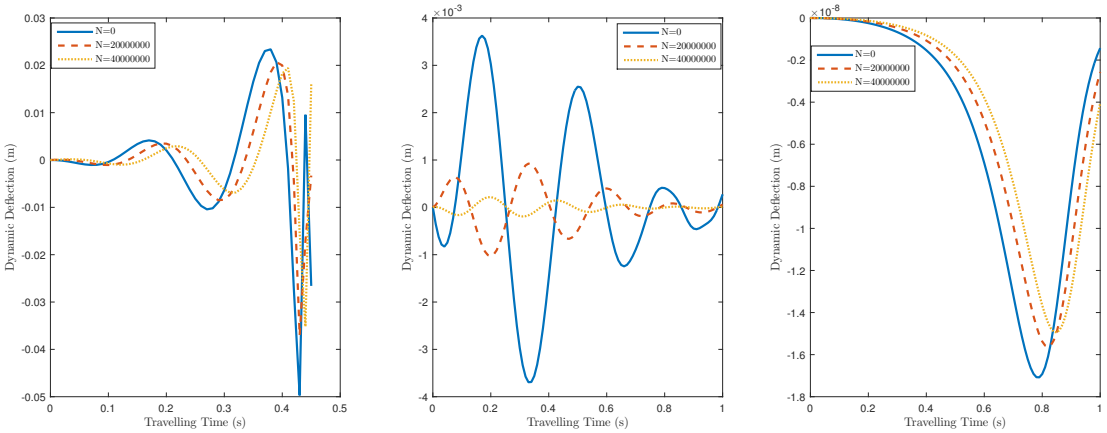

(a) accelerated motion ($\alpha > 0$) (b) decelerated motion ($\alpha < 0$) (c) uniform motion ($\alpha = 0$)

Figure 19: Deflection profiles of a fixed-free prismatic Rayleigh beam under accelerating masses; for fixed values of foundation modulus K = 40000, shear modulus G = 30000, and rotatory inertial $R_0 = 20$; and varied values of axial force N

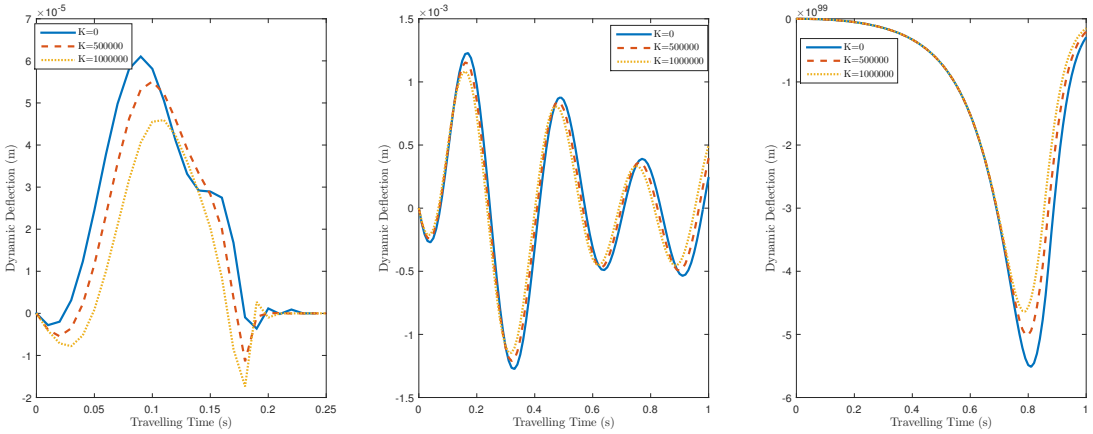

(a) accelerated motion ($\alpha > 0$) (b) decelerated motion ($\alpha < 0$) (c) uniform motion ($\alpha = 0$)

Figure 20: A fixed-free prismatic Rayleigh beam's transverse displacements under accelerating masses over a range of foundation modulus values K as well as fixed values of axial force N = 40000, shear modulus G = 30000, and rotatory inertial $R_0 = 20$.

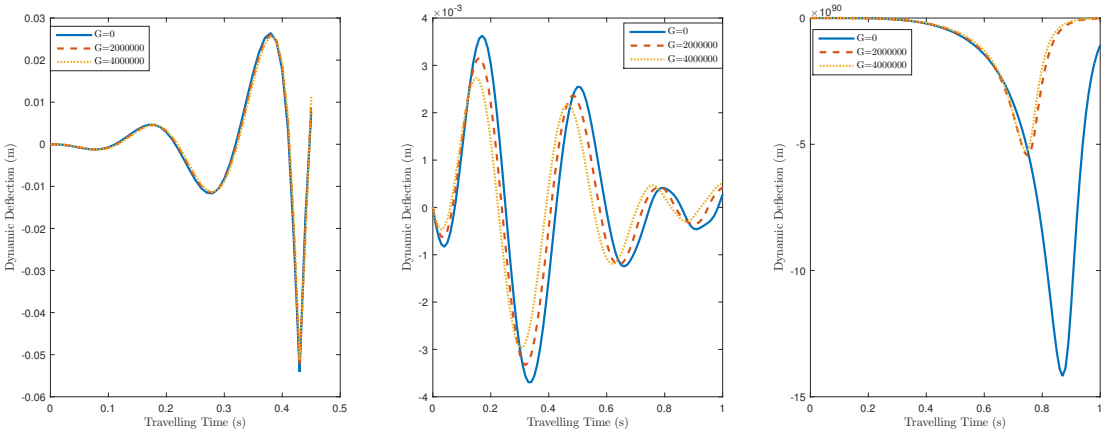

(a) accelerated motion ($\alpha > 0$) (b) decelerated motion ($\alpha < 0$) (c) accelerated motion ($\alpha = 0$)

Figure 21: Response amplitudes of a fixed-free prismatic Rayleigh beam under accelearting masses for various values of shear modulus G and for fixed values of axial force N = 20000 foundation modulus K = 40000, and rotatory inertial $R_0 = 20$

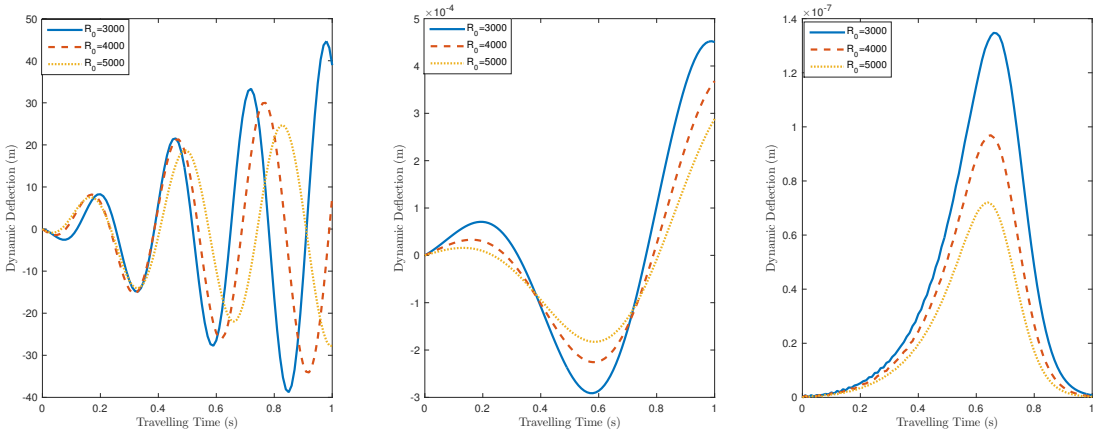

(a) accelerated motion ($\alpha > 0$) (b) decelerated motion ($\alpha < 0$) (c) uniform motion ($\alpha = 0$)

Figure 22: Deflection variations at the mid-span of a fixed-free prismatic Rayleigh beam under accelearting masses for various values of rotatory inertial factor R_0 and for fixed values of axial force N, foundation modulus K = 40000, shear modulus G = 30000

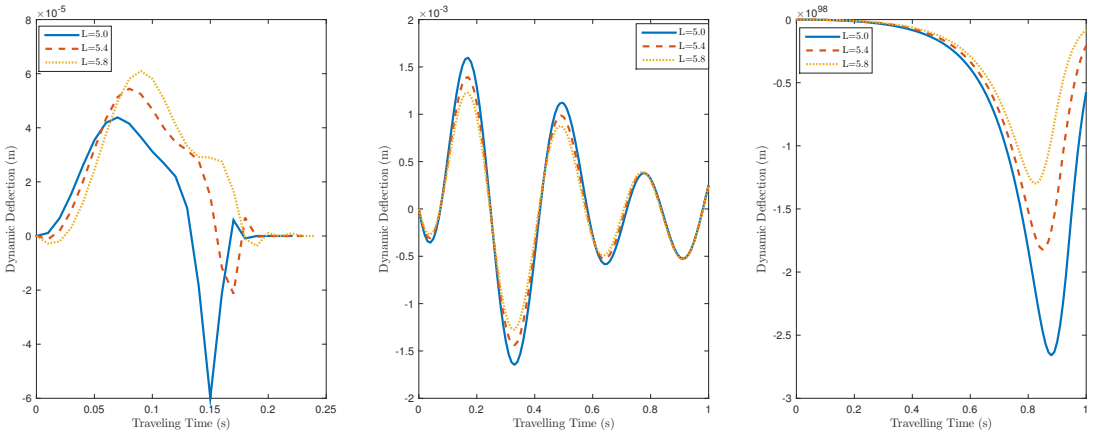

(a) accelerated motion ($\alpha > 0$) (b) decelerated motion ($\alpha < 0$) (c) uniform motion ($\alpha = 0$)

Figure 23: The present study examines the dynamic deflections of a fixed-free prismatic Rayleigh beam in relation to the crossing time of an accelerating mass, using different span length values L and fixed values of axial force N = 2000, foundation modulus K = 40000, shear modulus G = 30000, and rotatory inertial $R_0 = 20$.

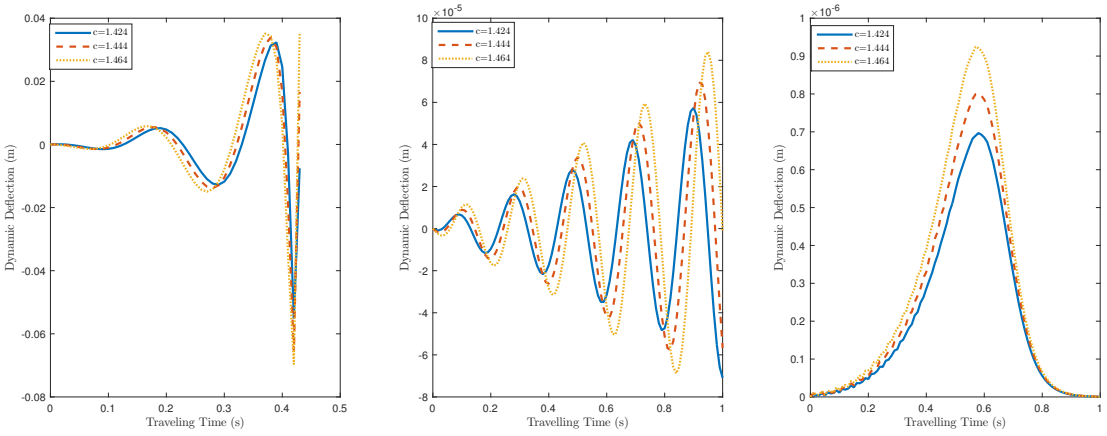

(a) accelerated motion ($\alpha > 0$) (b) decelerated motion ($\alpha < 0$) (c) uniform motion ($\alpha = 0$)

Figure 24: Plotting deflection curves against the crossing time of accelerating masses for a fixed-free prismatic Rayleigh beam with fixed values of axial force N = 2000, foundation modulus K = 40000, shear modulus G = 30000, and rotatory inertial factor $R_0 = 20$, for a range of travelling velocities.

5. Conclusions

This study investigated the response problem of a beam supported by a Pasternak foundation under varying velocity and arbitrary boundary conditions. The beams were either fixed-fixed or fixed-free. It is assumed that the beam is uniform, and the correction factor for rotatory inertia is included in the equation of motion that governs it. The system's bending movements are governed by fourth-order partial differential equations with varying coefficients that exhibit singularity. The Weighted Residual Method transforms these equations into coupled second-order ordinary differential equations. An asymptotic method developed by Struble was modified further to simplify the sequence of coupled second-order ordinary differential equations to obtain the second-order ordinary differential equations. The study utilized the Duhamel Integration Method, which involves impulse response functions, to obtain a solution representing a thick beam's transient dynamic response to accelerating partially distributed moving loads. The study used examples of structure-load systems with fixed and simple supports to establish how crucial structural parameters affect dynamic deflections. It provides insights into the dynamic characteristics of the beam when subjected to accelerating, decelerating, and uniform velocity types of motion. The results and analyses presented in this work align perfectly with previously published findings. It should be mentioned that the current study considers the flexural response of a Rayleigh beam with general boundary conditions. However, several real-life problems of beams can be modelled as a fourth-order partial differential equation with time-dependent boundary conditions. Hence, we hope to consider this class of problems in our future study.

Acknowledgement

Funding: Not applicable
Informed Consent Statement: Not applicable
Data Availability Statement: Not applicable

Conflict of interest statement

The author declares no potential conflict of interest.

References

[1] Salah EY, Sontakke B, Abdo MS, Shatanawi W, Abodayeh K, Albalwi MD. Conformable Fractional-Order Modeling and Analysis of HIV/AIDS Transmission Dynamics. International Journal of Differential Equations. 2024; 2024(1): 1958622.https://doi.org/10.1155/2024/1958622

[2] Awadalla M, Abuasbeh K, Noupoue YYY, Abdo MS. Modeling Drug Concentration in Blood through Caputo-Fabrizio and Caputo Fractional Derivatives. CMES-Computer Modeling in Engineering & Sciences. 2023; 135(3): 2767-2785. https://doi.org/10.32604/cmes.2023.024036

[3] Abidemi A, Alnegga M, Alade TO. A nonlinear mathematical model for exploring the optimal cost-effective therapeutic strategies and within-host viral infections spread dynamics. Healthcare Analytics. 2024; 5: 100321. https://doi.org/10.1016/j.health.2024.100321

[4] Abidemi A, Peter OJ, others. An optimal control model for dengue dynamics with asymptomatic, isolation, and vigilant compartments. Decision Analytics Journal. 2024: 100413. https://doi.org/10.1016/j.dajour.2024.100413

[5] Abidemi A, Owolabi KM. Unravelling the dynamics of Lassa fever transmission with nosocomial infections via nonfractional and fractional mathematical models. The European Physical Journal Plus. 2024; 139(2): 1-30.
[6] Adeloye TO. Dynamic Characteristics of a Simply Supported Beam Subjected to Compressive Axial Force and Impact Loads. International Journal of Maritime and Interdisciplinary Research. 2024; 4(2): 203-220.
[7] Abdelghany, S., Ewis, K., Mahmoud, A., and Nassar, M. (2015, sep). Dynamic response of non-uniform beam subjected to moving load and resting on non-linear viscoelastic foundation. Beni-Suef University Journal of Basic and Applied Sciences, 4(3), 192-199. doi:10.1016/j.bjbas.2015.05.007
[8] Adeoye SA, Adeloye TO. On the Dynamic Characteristics of Orthotropic Rectangular Plates under the Influence of Moving Distributed Masses and Resting on aVariable Elastic Pasternak Foundation. Journal of Material Science and Manufacturing Research. 2024; 5(1): 1-19.
[9] Adeoye SA, Adeloye TO. Response to Simply Supported Orthotropic Rectangular Plate Resting on a Variable Elastic Bi-Parametric Foundation under the Action of Moving Distributed Masses. Global Journal of Science Frontier Research. 2020;20.
[10] Abu-Hilal, M. (2003, jan). Vibration of beams with general boundary conditions due to a moving random load. Archive of Applied Mechanics (Ingenieur Archiv), 72(9), 637-650. doi:10.1007/s00419-002-0228-7
[11] Fr´yba, L. (1972). Vibration of solids and structures under moving loads. Springer Netherlands. doi:10.1007/978-94-011-9685-7
[12] He,W., and Wei, Y. (2019, mar). Dynamic response of double elastic cantilever beam attributed to variable uniformly distributed load. Mathematical Problems in Engineering, 2019, 1-17. doi:10.1155/2019/2657271
[13] Lu, T., Metrikine, A., and Steenbergen, M. (2020, nov). The equivalent dynamic stiffness of a viscoelastic halfspace in interaction with a periodically supported beam under a moving load. European Journal of Mechanics - A/Solids, 84, 104065. doi:10.1016/j.euromechsol.2020.104065
[14] Omolofe B and Adeloye TO. Behavioral study of finite beam resting on elastic foundation and subjected to travelling distributed masses. Latin American Journal of Solids and Structures. 2017; 14: 312-334.
[15] Omolofe B, Awodola T, Adeloye T. Damping influence on the critical velocity and response characteristics of structurally prestressed beam subjected to travelling harmonic load. Math Nat Sci Int J. 2018; 3: 18-28.
[16] Wang, R-T., and Chou, T-H. (1998, nov). Non-linear vibration of timoshenko beam due to a moving force and the weight of beam. journal of sound and vibration. Journal of Sound and Vibration, 218(1), 117-131. doi:10.1006/jsvi.1998.1827
[17] Oni, ST., and Omolofe, B. (2011, apr). Dynamic response of prestressed rayleigh beam resting on elastic foundation and subjected to masses traveling at varying velocity. Journal of Vibration and Acoustics, 133(4). doi:10.1115/1.4003405
[18] Omolofe, B., and Adara, EO. (2020, jan). Response characteristics of a beam-mass system with general boundary conditions under compressive axial force and accelerating masses. Engineering Reports, 2(2). doi:10.1002/eng2.12118
[19] Stanišić, MM., Euler, JA., and Montgomery, ST. (1974, sep). On a theory concerning the dynamical behavior of structures carrying moving masses. Ingenieur-Archiv, 43(5), 295-305. doi:10.1007/bf00537218
[20] Qiao, G., and Rahmatalla, S. (2021, jan). Dynamics of euler-bernoulli beams with unknown viscoelastic boundary conditions under a moving load. Journal of Sound and Vibration, 491, 115771. doi:10.1016/j.jsv.2020.115771
[21] Xu, Y., and Wang, N. (2020). Transverse free vibration of euler-bernoulli beam with pre-axial pressure resting on a variable pasternak elastic foundation under arbitrary boundary conditions. Latin American Journal of Solids and Structures, 17(7).doi:10.1590/1679-78256150
[22] Uzzal, RUA., Bhat, RB., and Ahmed, W. (2012). Dynamic response of a beam subjected to moving load and moving mass supported by pasternak foundation. Shock and Vibration, 19(2), 205-220. doi:10.1155/2012/919512